applied sciences

MDPI

Article

A Temperature Fiber Sensor Based on Tapered Fiber Bragg Grating Fabricated by Femtosecond Laser

Wen Zhang [1,2], Lianqing Zhu [1,2,*], Mingli Dong [1,2,*], Xiaoping Lou [1,2] and Feng Liu [1,2]

1 Beijing Laboratory of Optical Fiber Sensing and System, Beijing Information Science & Technology University, Beijing 100016, China; baswen@163.com (W.Z.); louxiaoping@bistu.edu.cn (X.L.); liufeng@bistu.edu.cn (F.L.)
2 Overseas Expertise Introduction Center for Discipline Innovation ("111 Center"), Beijing Information Science & Technology University, Beijing 100192, China
* Correspondence: zhulianqing@bistu.edu.cn (L.Z.); dongml@bistu.edu.cn (M.D.); Tel.: +86-10-8417-6477 (L.Z.)

Received: 10 October 2018; Accepted: 10 December 2018; Published: 14 December 2018

check for updates

Abstract: A temperature fiber sensor based on tapered fiber Bragg grating (tapered FBG) fabricated by femtosecond laser has been proposed and realized with good reproducibility. Firstly, the fiber taper with 25 μm diameter and 1000 μm length is fabricated by arc-discharge elongation using two standard single-mode fibers. Secondly, two first-order FBGs are fabricated in tapered and non-tapered fiber regions for comparison. Both FBGs are point-by-point direct-written by femtosecond laser, and the grating lengths are 1000 μm. Thirdly, a temperature experiment is performed using a heating chamber, and experimental results show that in the range of 30~350 °C, the temperature sensitivity of the tapered FBG has increased from 11.0 pm/°C to 12.3 pm/°C. The tapered FBG proposed here can be further configured for sensing other parameters in physical, chemical, and biomedical applications.

Keywords: tapered optical fiber sensor; fiber Bragg grating; temperature sensing; femtosecond laser fabrication

1. Introduction

Over the decades, optical fiber sensors have attracted growing interest for various applications, since they offer advantages including their small size, light weight, electromagnetic immunity, high stability, and the possibility of remote interrogation in sensor arrays [1]. These advantages are suitable for safe and efficient structural health monitoring and control. Examples where temperatures need to be accurately measured include biomedical cell culture and transformation, chemical and biological microfluidic systems, down-hole drillings for oil and gas exploration, and aircraft engines [2–4]. Therefore, a large variety of fiber optic temperature sensors have been envisioned and demonstrated for accurate temperature measurement. The sensitive structures include the fiber Bragg grating (FBG) [5–7], long period fiber grating (LPFG) [8], Fabry-Perot cavity [9–11], Mach-Zehnder interferometer [12–14], microfiber-based structures [3,15], etc.

Among these fiber sensing structures, FBG has narrow band filtering characteristics at certain wavelengths, which guarantees the desired precision for fiber sensing, fiber laser, and fiber communication. FBG is a periodic refractive index modulation along the optical fiber, which can be fabricated by exposing the fiber to an intense periodic optical laser. Generally, FBGs are created in photo-sensitive glass using ultraviolet laser, in which case, hydrogen loading is preferred for enhanced photosensitivity, since pure silica is non-photosensitive [16,17]. This inconvenience is challenging to realizing a complex grating structure as well as to expand the practical functions. However, femtosecond laser can remain efficient in fabricating non-photosensitive optical materials, which exhibits obvious advantages in FBG fabrication [18–22]. The femtosecond laser interacts with dielectric material through a high nonlinear photoionization mechanism, leading to the modification which shares no relevance to the photosensitivity of the material [23–28].

As for sensitivity-intensified fiber structures, a tapered fiber region exposes more contacting areas to the ambient and enhances the evanescent field, thus improving the sensitivity to external parameters more than conventional non-tapering optical fiber, which is very important for achieving heat monitoring and control more precisely and efficiently [15,29–32].

Relevant literatures have been reported in the past few years. Particularly, in 2013, Y. Ran et al. [33] reported a temperature-compensated refractive-index sensor using a single FBG in an abrupt fiber taper. The taper diameter is 12 μm and the taper length is 10 mm. The FBG were inscribed in the tapered region using a 193 nm ArF excimer laser and a phase mask with period of 1089.2 nm. With such a diameter–length ratio in the tapered region, the sensor had three different peaks for a single FBG, and the temperature characterization was used for measurement compensation. In 2017, D. Sun et al. [34] reported a label-free detection of cancer biomarkers using an in-line taper fiber-optic interferometer and a FBG. The FBG was inscribed in a standard fiber using a 193 nm ArF excimer laser and a phase mask with a period of 1070.49 nm, and the taper was later drawn near the FBG. The temperature sensitivities for taper and FBG were 10.7 pm/°C and 9.5 pm/°C, respectively. In 2018, A. D. Gomes et al. [35] reported a temperature-independent refractive index measurement using a FBG on an 18 μm diameter abrupt tapered tip. The FBG was inscribed in the tapered region using an 267 nm femtosecond laser and a phase mask with a period of 1075 nm. The taper was then broken at one of the transition regions in order to create the tip. The temperature sensitivity for the higher-order mode is 9.6 ± 0.1 pm/°C and that for the fundamental mode is 10.0 ± 0.1 pm/°C. However, in the literature, the point-by-point direct-written FBG by femtosecond laser in a fiber-tapered region has not yet been reported.

Here we propose a FBG fabricated by femtosecond laser inscribed in a fiber taper. The temperature-sensing experiment is performed by monitoring the characterized wavelengths under different temperatures. Such a tapered FBG will have applications in sensing physical, chemical and biomedical parameters.

2. Sensor Structure and Principle

A FBG is a periodic and permanent modification of the core refractive index value along the optical fiber axis. The FBG inscription is defined by the Bragg phase matching condition [34]:

$$m\lambda_B = 2n_{eff}\Lambda \tag{1}$$

where m is the order number, λ_B is the Bragg resonance wavelength, n_{eff} represents the effective index of the fiber core, and Λ is the grating pitch. Temperature affects the Bragg wavelength shift through the thermal expansion and the thermo-optical effect, which can be expressed by:

$$S_T = \frac{d\lambda_B}{dT} = \lambda_B(\alpha + \beta) \tag{2}$$

where $\alpha = \frac{1}{\Lambda} \cdot \frac{d\Lambda}{dT} \sim 0.55 \times 10^{-6}/°C$ is the thermal expansion coefficient; $\beta = \frac{1}{n_{eff}} \cdot \frac{dn_{eff}}{dT} \sim 6 \times 10^{-6}/°C$ is the thermo-optic coefficient of the optical fiber.

The proposed tapered-FBG and its light propagation are illustrated in Figure 1. In principle, a tapered FBG is a special version of a standard fiber Bragg grating. The tapered fiber region contains two transition regions, where the fiber diameter gradually decreases and then increases. When the light propagates in the optical fiber, the energy inside the fiber core is constrained within by reflective boundary conditions. When the incident broadband light travels along the fiber core and arrives at the FBG, there will be a high back reflection only at the Bragg wavelength λ_B.

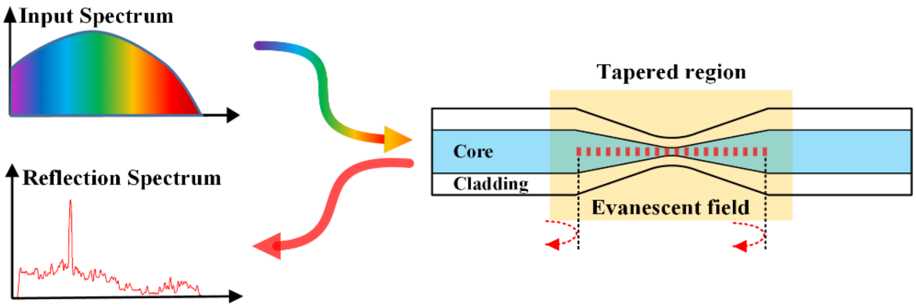

Figure 1. Light propagation and interference mode of the proposed tapered FBG.

Meanwhile, the rest energy will be transmitted along the tapered region, namely an evanescent field. In a standard non-tapered fiber, modes are confined by the core/cladding interface. While in the tapered region, light is initially focused in the thinning core until core guidance becomes so weak that the mode expands, then the mode is guided by the cladding/air interface, and here the mode diameter is at its maximum. The mode is then confined by the cladding/air interface and reveals the maximum confinement, which makes the tapered structure more sensitive than common cylinder geometry.

It has been demonstrated that the sensitivity of the tapered fiber is largely determined by its geometrical parameters, especially the taper lengths and diameters [3,15,33]. The tapered region is particularly important for sensing applications as it allows maximum interaction with the surroundings, and thus it has predictable compactness and sensitivity improvement.

3. Device Fabrication

As mentioned above, the optical fiber taper is a crucial component for temperature sensitivity improvement. The taper, with 25 μm diameter waist and 1000 μm length, was fabricated using a commercial fusion splicer (80S, Fujikura Ltd., Tokyo, Japan). In our experiment, the taper with relatively short and asymmetrical transition regions is preferred. Here we propose a reliable and effective method of fabricating an asymmetrical taper using a basic fusion splicer from two identical optical fibers. In order to ensure that the taper will have the required spectral properties, which can be further optimized for specific sensing applications, the transmission spectrum of the fiber taper was monitored during the whole tapering procedure.

Firstly, the fiber coatings of two standard single-mode fibers (SMF-28e+, Corning Ltd., New York, NY, USA) were wiped out at about 10 mm and were cleaved flat. Then the fiber taper was fabricated by elongating it during an arc-discharge provided by the fusion splicer. A constant tension was applied to the fiber throughout the whole tapering procedure, which results in the asymmetric taper profile. The waist diameter and the length of the fiber taper are controlled by adjusting the discharge current, the duration time and pre-stress. As in this procedure, using a lower discharge intensity is likely to obtain a longer taper with a thinner waist, however, it is more fragile. After comparison, the discharge intensity was set to −50 bit (bit is a default unit of discharge intensity of the fusion splicer) and the arc time was set to 900 ms in the tapering procedure. Finally, the fiber taper with 25 μm diameter and 1000 μm length was fabricated, where the FBG will later be inscribed on. The microscopic image of the fiber taper before inscription is shown in Figure 2, which was obtained from a commercial microscope (WDK2010-Z, Cewei Guangdian Ltd., Shanghai, China).

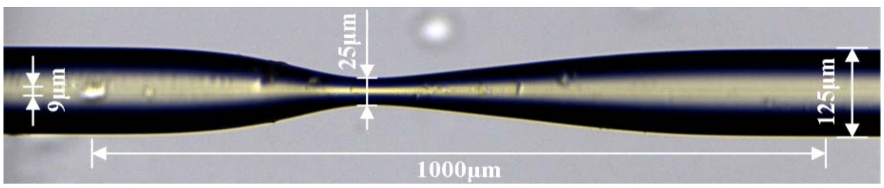

Figure 2. Microscopic image of the fiber taper (10x, NA = 0.3).

The schematic of the experimental setup for FBG inscription on the tapered fiber region by femtosecond laser is shown in Figure 3, which includes a femtosecond laser system (Astrella, Coherent Inc., Santa Clara, CA, USA), a broadband amplified spontaneous emission (ASE) source (MPD-3303, Mywave Instrument Co. Ltd., Shenzhen, China), and an optical spectrum analyzer (AQ6370D, Yokogawa Test & Measurement Corporation, Tokyo, Japan). The inscription process can be observed through the microscope objective lens. The motorized two-dimensional translation stage is used to keep the fiber axis coinciding with the laser focus. A circulator is used for light propagation. The broadband light source could offer light in the experiment. The OSA is used to observe the evolution of the FBG reflection spectrum during the grating inscription.

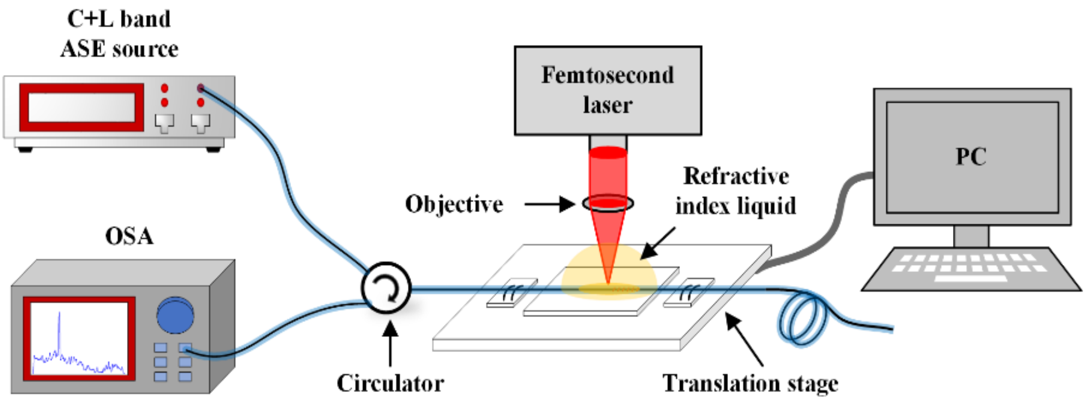

Figure 3. Experimental setup for FBG inscription on tapered fiber by femtosecond laser.

Experimentally, a Ti: Sapphire amplifier laser system (Astrella, Coherent Inc., Santa Clara, CA, USA) with an operation wavelength of 800 nm, pulse duration of 35 fs, and a laser repetition rate of 1 kHz was adopted. To precisely control the refractive index modulation, the laser beam was firstly filtered through a pin-hole to form a smooth Gaussian beam with the diameter adjusted to 4 mm. Then, the laser beam was focused into the taper through a high numerical aperture oil-immersion objective (Plan-Apochromat, Zeiss, Oberkochen, Germany). The femtosecond laser fabrication platform is shown in Figure 4, where the two-dimensional translation stage XMS100, (Newport Industries Ltd., Miami, FL, USA) is controlled by PC. In order to avoid the focus distortion caused by the fiber cylindrical lens effect, the fiber is immersed in the refractive index liquid drops. During the inscription, both the objective and the fiber were immersed in the liquid, which can be observed from the faint halo as well as the bright reflection, as shown in Figure 4.

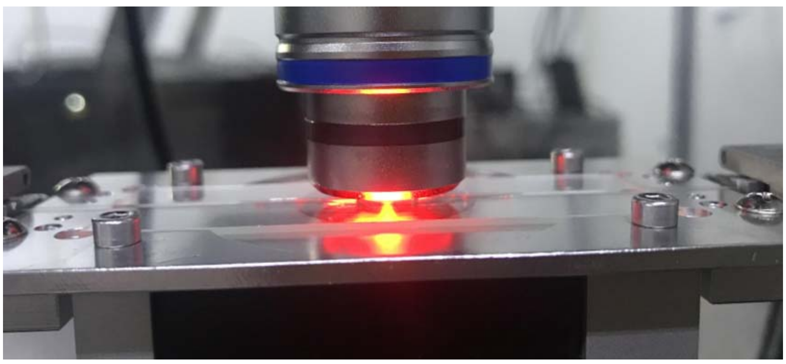

Figure 4. Femtosecond laser fabrication platform.

Before the tapered FBG inscription, a FBG was fabricated 10 mm away from the taper in a non-tapered fiber region for comparison. The reference FBG is first-order and point-by-point written by femtosecond laser. The grating pitch is 550 nm, and the grating length is 1000 μm.

Then the tapered-FBG was inscribed by femtosecond laser in the tapered region using the point-by-point direct-writing method, and the inscription details in the thinnest waist are shown in Figure 5, which were directly obtained from the inscription objective. The grating pitch is 535 nm, and the grating length is 1000 μm. From Figure 5, the taper profile, fiber core, fiber cladding, and inscription trace can be clearly noticed.

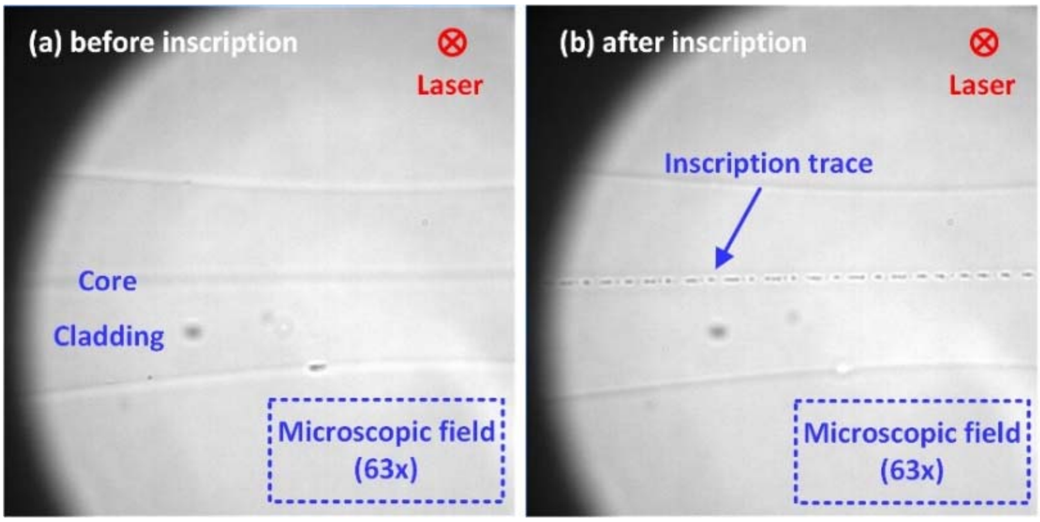

Figure 5. Inscription details of the proposed sensor using femtosecond laser in the taper region.

The reflection spectra evolution before and after the tapered FBG fabrication were recorded by an OSA (AQ6370D, Yokogawa Test & Measurement Corporation, Tokyo, Japan) with a resolution of 0.5 nm, as shown in Figure 6. The characterized Bragg wavelength of the tapered FBG is chosen as peak A. The characterized Bragg wavelengths of the reference FBG before and after the tapered FBG are chosen as peak C and B, respectively. Relevant peak information is listed in Table 1.

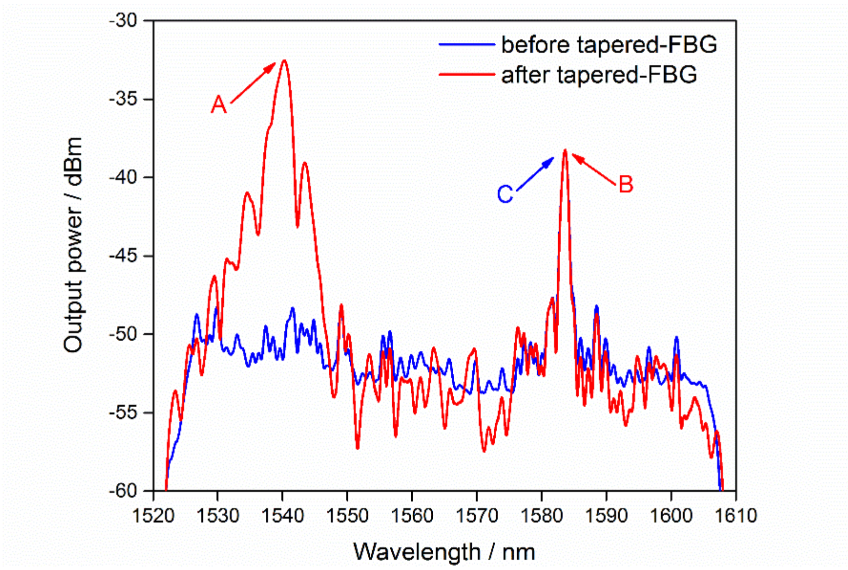

Figure 6. Reflection spectra before and after the tapered FBG fabrication.

According to Figure 6 and Table 1, the comparison of the -3 dB fractional bandwidths between the tapered FBG and the reference FBG shows that due to the special geometry and mode propagation, the tapered-FBG has a wider bandwidth appearance. Also, it can be noticed that after the tapered FBG was fabricated, there is a minor fluctuation of the refection spectrum covering the whole C+L bandwidth. Moreover, the Bragg wavelengths, the output powers and the −3 dB fractional bandwidths of the reference FBG before and after the tapered-FBG inscription remain almost the same, which means that the reference FBG hardly suffers from the inscription interference.

Table 1. FBG information of the reflection spectra evolution.

Peak Index	Grating Pitch (nm)	Grating Length (μm)	Wavelength (nm)	Output Power (dBm)	−3 dB Fractional Bandwidth (nm)
A	535	1000	1540.25	−32.54	2.75
B	550	1000	1583.62	−38.25	1.12
C	550	1000	1583.62	−38.28	1.13

4. Results and Discussion

In the following analysis, peak A (1540.25 nm) and peak B (1583.62 nm) are chosen for comparison. The temperature experiment is performed in the class-1000 cleanroom and the temperature-sensing system is shown in Figure 7. Inside the furnace chamber, there is a platform. When the sensor is under the temperature test, it is placed on the upper surface of the platform without fixation. There are two drilling holes on the front and back furnace doors, which could support the optical fiber yet without strain applied on the proposed sensor. The reflection spectra are monitored during the temperature experiment. Both the heating and cooling processes are tested. The temperature range provided by the heating chamber is from 30 °C to 350 °C, and the reflection spectra is recorded by a step of 10 °C. Each reflection spectrum is measured after 20 min staying at a specific temperature to guarantee thermal equilibrium.

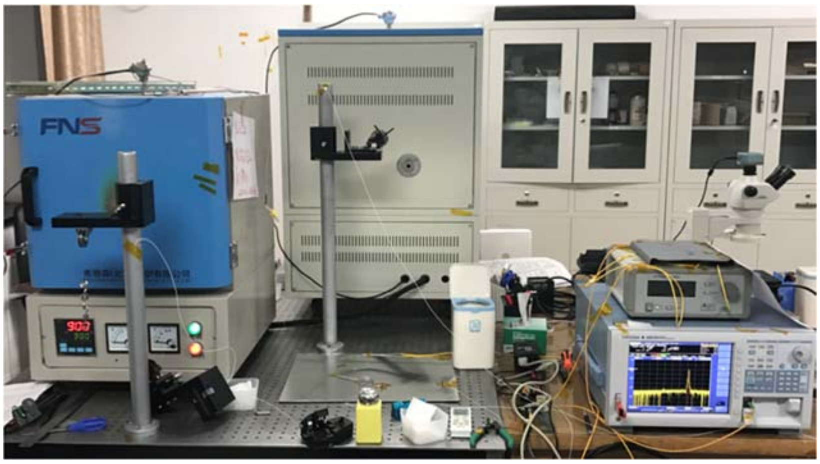

Figure 7. Temperature-sensing system.

Figure 8 shows the wavelength shifts of the tapered FBG and the reference FBG (peak A and B) with the temperature variation. For clarity, the spectra from 1520 nm to 1610 nm at 30 °C and 350 °C are demonstrated in Figure 8a. The detailed reflection spectra of peak A and B are demonstrated in Figure 8b–e. For clarity, the spectra are exhibited every 20 °C. The temperature sensitivity analyses of both FBGs are shown in Figure 8f.

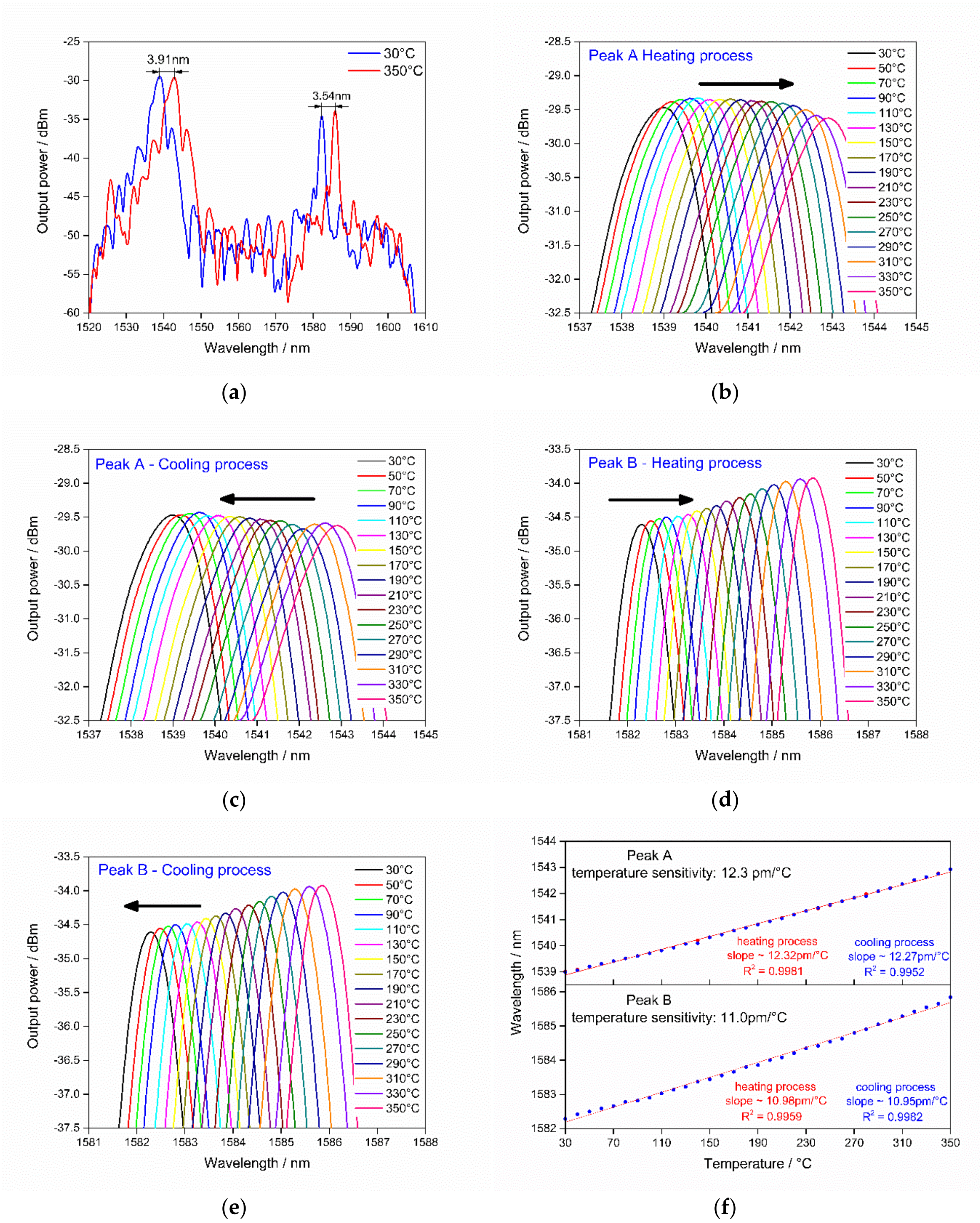

Figure 8. Reflection spectra and temperature-sensitivity analysis of the proposed sensor. (**a**) Reflection spectra at 30 °C and 350 °C for comparison; (**b**) Detailed reflection spectra of peak A during the heating process from 30 °C to 350 °C; (**c**) Detailed reflection spectra of peak A during the cooling process from 350°C to 30 °C; (**d**) Detailed reflection spectra of peak B during the heating process from 30 °C to 350 °C; (**e**) Detailed reflection spectra of peak B during the cooling process from 350 °C to 30 °C; (**f**) Temperature characterization of peak A and B.

It can be seen in Figure 8 that the characterized wavelengths of the tapered FBG and the reference FBG shift when the temperature increases, yet with different wavelength variations. When temperature increases from 30 °C to 350 °C, red shifts happen for both FBGs. When the temperature decreases from 350 °C to 30 °C, blue shifts happen for both FBGs. From Figure 8a, the wavelength variation of the tapered FBG in the 30–350 °C range is 3.91 nm, while that of the reference FBG is 3.54 nm. This is because the tapered FBG exposes more to the ambient, resulting in a more sensitive wavelength variation. According to Figure 8b–e, both FBGs shift linearly along with the temperature change.

For further discussion, the temperature-wavelength relationships of both FBGs are analyzed in Figure 8f. For each FBG, the characterized wavelengths at specific temperatures in the heating and cooling processes are shown in one subfigure. The experimental results are marked in blue or red circles, and the linear fitting evaluation is used to obtain the sensitivities, where the slope represents the temperature sensitivity and the R-square represents the fitting evaluation. As shown in Figure 8f, both FBGs demonstrate good linearity along with the temperature variation, and R-squares are quite satisfactory. For accuracy, the round-up temperature sensitivities are used. Compared to the reference FBG fabricated by femtosecond laser, the temperature sensitivity of the tapered FBG has improved from 11.0 pm/°C to 12.3 pm/°C.

In order to discuss the reproducibility of the technique, we fabricated five tapered FBGs for comparison using the same fabrication conditions. The Fujikura 80S was used to fabricated fiber tapers with 25 μm diameter and 1000 μm length. For the femtosecond laser inscription, all of the five tapered FBGs were first order with grating pitches being 535 nm and grating lengths being 1000 μm. Then the temperature behaviors of the five tapered FBGs were investigated in the aforementioned furnace chamber with a test temperature range of 30–350 °C. All five tapered FBGs exhibited a red shift during the heating processes, and a blue shift during the cooling processes. The Bragg wavelengths and temperature sensitivities of the five tapered FBGs are listed in Table 2.

Table 2. Bragg wavelengths and temperature sensitivities of the five tapered FBGs.

FBG Index	Grating Pitch (nm)	Grating Length (μm)	Bragg Wavelength (nm)	Temperature Sensitivity		
				Heating Process (pm/°C)	Cooling Process (pm/°C)	Mean Result (pm/°C)
1	535	1000	1540.25	12.32	12.27	12.30
2	535	1000	1540.25	12.17	12.10	12.14
3	535	1000	1540.24	12.34	12.07	12.21
4	535	1000	1540.25	12.13	11.99	12.06
5	535	1000	1540.23	12.35	11.96	12.16

Notably, the temperature fiber sensors based on first-order tapered-FBGs can be fabricated by femtosecond laser with good reproducibility. Combined with the experimental data in Table 2, the Bragg wavelengths can be precisely controlled given the grating pitch and the length on the same kind of optical fiber. During cooling processes, the temperature sensitivities are slightly smaller compared to those in the heating processes. This is probably due to the fact that the thermal equilibrium takes longer during the cooling process. By prolonging the stabling period, the associated errors can be further improved.

5. Conclusions

In conclusion, a tapered temperature fiber sensor based on FBG fabricated by femtosecond laser has been proposed and realized with good reproducibility. By arc-discharge elongation using two standard single-mode fibers, the fiber taper with 25 μm diameter and 1000 μm length was fabricated. A reference FBG was inscribed 10 mm away from the fiber taper for comparison, and then the tapered-FBG was inscribed in the aforementioned taper. Both FBGs are first-order, point-by-point direct-written, and each grating length is 1000 μm. The grating pitches of the tapered FBG and the reference FBG are 535 nm and 550 nm, respectively. The characterized wavelengths of the tapered FBG and reference FBG are 1540.25 nm and 1583.62 nm, respectively. The temperature experimental results show that in the range of 30–350 °C, the temperature sensitivity of the tapered FBG has increased from 11.0 pm/°C to 12.3 pm/°C. In future, a greater improvement in temperature sensitivity could be achieved by optimizing the taper profile as well as the femtosecond laser fabrication technique, which may further promote this proposal to be successfully implemented for sensing other parameters in physical, chemical, and biomedical applications.

Author Contributions: Conceptualization, W.Z.; Data curation, X.L.; Methodology, L.Z. and M.D.; Software, F.L.; Validation, W.Z.; Writing—original draft, W.Z.

Funding: This research was funded by Changjiang Scholars and Innovative Research Team in University (No. IRT_16R07), Importation and Development of High-Caliber Talents Project of Beijing Municipal Institutions (No. IDHT20170510), National Natural Science Foundation of China (No. 61801030), and General Project of the Science and Technology Program of Beijing Municipal Education Commission (No. KM201811232008).

Acknowledgments: The authors would like to acknowledge the research and technical support given by Beijing Laboratory of Optical Fiber Sensing and System, and Overseas Expertise Introduction Center for Discipline Innovation ("111 Center").

Conflicts of Interest: The authors declare no conflict of interest.

References

1. Antonio-Lopez, J.E.; Eznaveh, Z.S.; LiKamWa, P.; Schulzgen, A.; Amezcua-Correa, R. Multicore fiber sensor for high-temperature applications up to 1000 °C. *Opt. Lett.* **2014**, *39*, 4309–4312. [CrossRef] [PubMed]
2. di Sante, R. Fibre Optic Sensors for Structural Health Monitoring of Aircraft Composite Structures: Recent Advances and Applications. *Sensors* **2015**, *15*, 18666–18713. [CrossRef] [PubMed]
3. Yan, S.; Xu, F. A review on optical microfibers in fluidic applications. *J. Micromech. Microeng.* **2017**, *27*, 093001. [CrossRef]
4. Arjmand, M.; Saghafifar, H.; Alijanianzadeh, M.; Soltanolkotabi, M. A sensitive tapered-fiber optic biosensor for the label-free detection of organophosphate pesticides. *Sens. Actuators B Chem.* **2017**, *249*, 523–532. [CrossRef]
5. Li, Y.; Liao, C.; Wang, D.N.; Lu, J.; Lu, P. Fiber Bragg Grating for High Temperature Applications. In Proceedings of the 15th OptoElectronics and Communications Conference (OECC2010) Technical Digest Sapporo Convention Center, Sapporo, Japan, 5–9 July 2010.
6. Jiang, Y.; Liu, C.; Li, D.; Yang, D.; Zhao, J. Simultaneous measurement of temperature and strain using a phase-shifted fiber Bragg grating inscribed by femtosecond laser. *Meas. Sci. Technol.* **2018**, *29*, 045101. [CrossRef]
7. Ding, M.; Yang, B.; Jiang, P.; Liu, X.; Dai, L.; Hu, Y.; Zhang, B. High-sensitivity thermometer based on singlemode-multimode FBG-singlemode fiber. *Opt. Laser Technol.* **2017**, *96*, 313–317. [CrossRef]
8. Zhang, W.; Hao, J.; Lou, X.; Dong, M.; Zhu, L. All-Fiber Dual-Parameter Sensor Based on Cascaded Long Period Fiber Grating Pair Fabricated by Femtosecond Laser and CO_2 Laser. *Fiber Integr. Opt.* **2018**, *37*, 66–78. [CrossRef]
9. Xiang, Y.; Luo, Y.; Li, Y.; Li, Y.; Yan, Z.; Liu, D.; Sun, Q. Quasi-Distributed Dual-Parameter Optical Fiber Sensor Based on Cascaded Microfiber Fabry–Perot Interferometers. *IEEE Photonics J.* **2018**, *10*, 2400309. [CrossRef]
10. Zhang, X.; Peng, W.; Shao, L.; Pan, W.; Yan, L. Strain and temperature discrimination by using temperature-independent FPI and FBG. *Sens. Actuators A Phys.* **2018**, *272*, 134–138. [CrossRef]
11. Theodosiou, A.; Hu, X.; Caucheteur, C.; Kalli, K. Bragg Gratings and Fabry-Perot Cavities in Low-Loss Multimode CYTOP Polymer Fiber. *IEEE Photonics Technol. Lett.* **2018**, *30*, 857–860. [CrossRef]
12. Liao, C.R.; Wang, Y.; Wang, D.N.; Yang, M.W. Fiber In-Line Mach–Zehnder Interferometer Embedded in FBG for Simultaneous Refractive Index and Temperature Measurement. *IEEE Photonics Technol.* **2010**, *22*, 1686–1688. [CrossRef]
13. Hu, Y.; Jiang, C.; Zhou, M.; Liu, J. High-sensitivity fiber temperature and refractive index sensing with nonadiabatic fiber taper. *J. Opt. Technol.* **2018**, *85*, 233–237. [CrossRef]
14. Tan, J.; Feng, G.; Zhang, S.; Liang, J.; Li, W.; Luo, Y. Dual spherical single-mode-multimode-single-mode optical fiber temperature sensor based on a Mach—Zehnder interferometer. *Laser Phys.* **2018**, *28*, 075102. [CrossRef]
15. Talataisong, W.; Ismaeel, R.; Brambilla, G. A Review of Microfiber-Based Temperature Sensors. *Sensors* **2018**, *18*, 461. [CrossRef]
16. Hoeffgen, S.K.; Henschel, H.; Kuhnhenn, J.; Weinand, U.; Caucheteur, C.; Grobnic, D.; Mihailov, S.J. Comparison of the Radiation Sensitivity of Fiber Bragg Gratings Made by Four Different Manufacturers. *IEEE Trans. Nucl. Sci.* **2011**, *58*, 906–909. [CrossRef]

17. O'Byrne, R.P.; Sergeyev, S.V.; Flavin, D.A.; Slattery, S.A.; Nikogosyan, D.N.; Jones, J.D.C. Anisotropic Fiber Bragg Gratings Inscribed by High-Intensity Femtosecond-UV Pulses: Manufacturing Technology and Strain Characterization for Sensing Applications. *IEEE Sens. J.* **2008**, *8*, 1256–1263. [CrossRef]
18. Zheng, Z.; Yu, Y.; Zhang, X.; Guo, Q.; Sun, H. Femtosecond Laser Inscribed Small-Period Long-Period Fiber Gratings with Dual-Parameter Sensing. *IEEE Sens. J.* **2018**, *18*, 1100–1103. [CrossRef]
19. Yang, K.; He, J.; Liao, C.; Wang, Y.; Liu, S.; Guo, K.; Zhou, J.; Li, Z.; Tan, Z.; Wang, Y. Femtosecond Laser Inscription of Fiber Bragg Grating in Twin-Core Few-Mode Fiber for Directional Bend Sensing. *J. Lightwave Technol.* **2017**, *35*, 4670–4676. [CrossRef]
20. Marchi, G.; Stephan, V.; Dutz, F.J.; Hopf, B.; Polz, L.; Huber, H.P.; Roths, J. Femtosecond Laser Machined Micro-Structured Fiber Bragg Grating for Simultaneous Temperature and Force Measurements. *J. Lightwave Technol.* **2016**, *34*, 4557–4563. [CrossRef]
21. Jiang, Y.; Liu, C.; Zhang, W.; Mao, D.; Yang, D.; Zhao, J. Multi-Parameter Sensing Using a Fiber Bragg Grating Inscribed in Dual-Mode Fiber. *IEEE Photonics Technol. Lett.* **2017**, *29*, 1607–1610. [CrossRef]
22. Chen, C.; Zhang, X.; Yu, Y.; Wei, W.; Guo, Q.; Qin, L.; Ning, Y.; Wang, L.; Sun, H. Femtosecond Laser-Inscribed High-Order Bragg Gratings in Large-Diameter Sapphire Fibers for High-Temperature and Strain Sensing. *J. Lightwave Technol.* **2018**, *36*, 3302–3308. [CrossRef]
23. Baghdasaryan, T.; Geernaert, T.; Becker, M.; Schuster, K.; Bartelt, H.; Makara, M.; Mergo, P.; Berghmans, F.; Thienpont, H. Influence of Fiber Orientation on Femtosecond Bragg Grating Inscription in Pure Silica Microstructured Optical Fibers. *IEEE Photonics Technol. Lett.* **2011**, *23*, 1832–1834. [CrossRef]
24. Zhou, K.; Dubov, M.; Mou, C.; Zhang, L.; Mezentsev, V.K.; Bennion, I. Line-by-Line Fiber Bragg Grating Made by Femtosecond Laser. *IEEE Photonics Technol. Lett.* **2010**, *22*, 1190–1192. [CrossRef]
25. Liao, C.; Li, Y.; Wang, D.N.; Sun, T.; Grattan, K.T.V. Morphology and Thermal Stability of Fiber Bragg Gratings for Sensor Applications Written in H2-Free and H2-Loaded Fibers by Femtosecond Laser. *IEEE Sens. J.* **2010**, *10*, 1675–1681. [CrossRef]
26. Donko, A.; Beresna, M.; Jung, Y.; Hayes, J.; Richardson, D.J.; Brambilla, G. Point-by-point femtosecond laser micro-processing of independent core-specific fiber Bragg gratings in a multi-core fiber. *Opt. Express* **2018**, *26*, 2039–2044. [CrossRef] [PubMed]
27. Theodosiou, A.; Lacraz, A.; Stassis, A.; Koutsides, C.; Komodromos, M.; Kalli, K. Plane-by-Plane Femtosecond Laser Inscription Method for Single-Peak Bragg Gratings in Multimode CYTOP Polymer Optical Fiber. *J. Lightwave Technol.* **2017**, *35*, 5404–5410. [CrossRef]
28. Grobnic, D.; Mihailov, S.J.; Smelser, C.W. Localized High Birefringence Induced in SMF-28 Fiber by Femtosecond IR Laser Exposure of the Cladding. *J. Lightwave Technol.* **2007**, *25*, 1996–2001. [CrossRef]
29. Lou, J.; Wang, Y.; Tong, L. Microfiber optical sensors: A review. *Sensors* **2014**, *14*, 5823–5844. [CrossRef]
30. Layeghi, A.; Latifi, H. Magnetic field vector sensor by a nonadiabatic tapered Hi-Bi fiber and ferrofluid nanoparticles. *Opt. Laser Technol.* **2018**, *102*, 184–190. [CrossRef]
31. Silva, S.; Coelho, L.; Almeida, J.M.; Frazao, O.; Santos, J.L.; Malcata, F.X.; Becker, M.; Rothhardt, M.; Bartelt, H. H2 Sensing Based on a Pd-Coated Tapered-FBG Fabricated by DUV Femtosecond Laser Technique. *IEEE Photonics Technol. Lett.* **2013**, *25*, 401–403. [CrossRef]
32. Zhu, F.; Zhang, Z.; Liao, C.; Wang, Y.; Xu, L.; He, J.; Wang, C.; Li, Z.; Yang, T.; Wang, Y. Taper Embedded Phase-Shifted Fiber Bragg Grating Fabricated by Femtosecond Laser Line-by-Line Inscription. *IEEE Photonics J.* **2018**, *10*, 1–8. [CrossRef]
33. Ran, Y.; Jin, L.; Sun, L.; Li, J.; Guan, B. Temperature-Compensated Refractive-Index Sensing Using a Single Bragg Grating in an Abrupt Fiber Taper. *IEEE Photonics J.* **2013**, *5*, 7100208.
34. Sun, D.; Ran, Y.; Wang, G. Label-Free Detection of Cancer Biomarkers Using an In-Line Taper Fiber-Optic Interferometer and a Fiber Bragg Grating. *Sensors* **2017**, *17*, 2559. [CrossRef] [PubMed]
35. Gomes, A.D.; Silveira, B.; Warren-Smith, S.C.; Becker, M.; Rothhardt, M.; Frazão, O. Temperature independent refractive index measurement using a fiber Bragg grating on abrupt tapered tip. *Opt. Laser Technol.* **2018**, *101*, 227–231. [CrossRef]